Lack of junctional adhesion molecule (JAM)-B traps CD8 T cells in the CNS borders and ameliorates autoimmune neuroinflammation

*Javier Pareja[1#&], Sidar Aydin[1# *], Mara Zbinden[1], Elisa Bouillet[1], Niklas Zollinger[1], Vidusiya Theivendram[1], Amal Fahmi[1], Petr Pleskač[1], Sara Barcos[1], Felix Paas[1], Florencia Kloster[1], Aida Muñoz Blázquez[1], Nicolas Fonta[2], Doron Merkler[2], Urban Deutsch[1], Britta Engelhardt[1]*

[1]Theodor Kocher Institute, University of Bern, Bern, Switzerland

[2]Department of Pathology and Immunology, Division of Clinical Pathology, University and University Hospitals of Geneva, Geneva, Switzerland

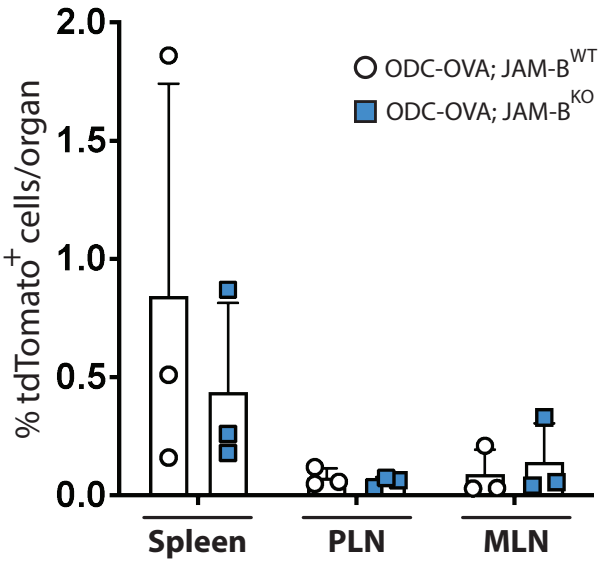
[#]Authors contributed equally

* Current address: Department of Pharmacology, University of California, San Diego, USA

[&] Current address: Department of Biomedicine, University of Basel, Basel, Switzerland

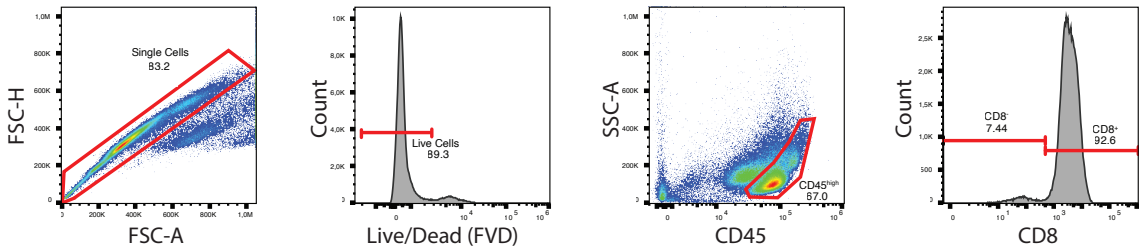
Corresponding authors:
Britta Engelhardt
E-Mail: britta.engelhardt@unibe.ch
Phone: + 41 31 684 4143

Javier Pareja
E-Mail: javier.pareja.roman@gmail.com
Phone: +34 637037322



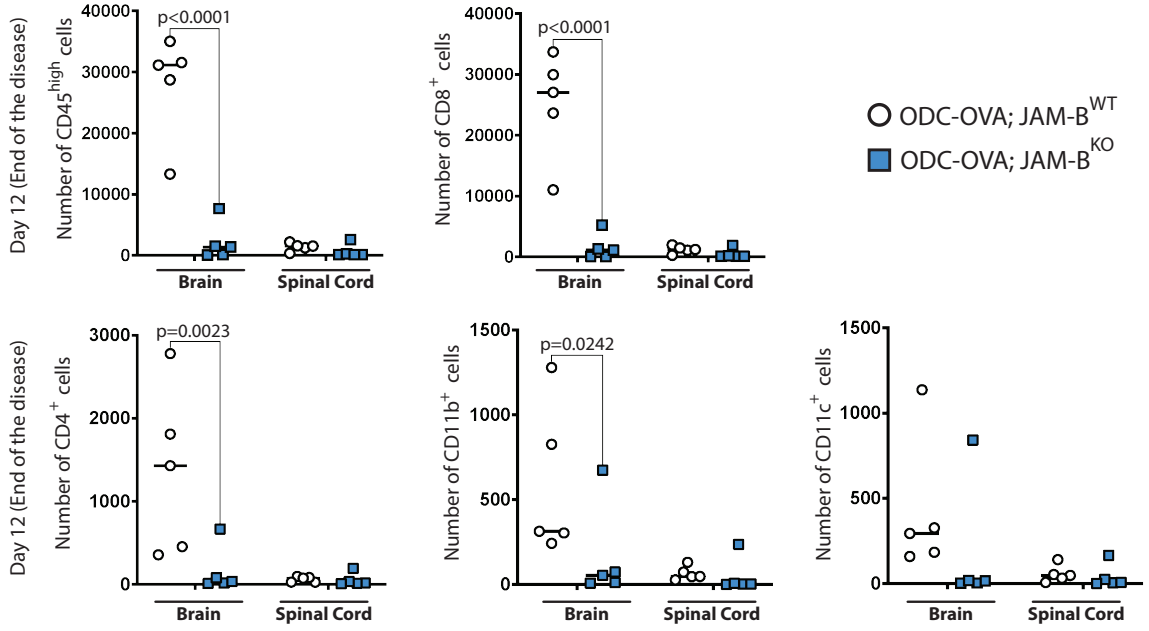
Supplementary Fig. 1 *In vivo* homing of *in vitro* activated CD8 T cells to peripheral lymphoid organs

ODC-OVA; JAM-B^{WT} and ODC-OVA; JAM-B^{KO} mice were adoptively transferred with 10^7 *in vitro* activated tdTomato$^+$ OT-I cells and the spleen, peripheral and mesenteric lymph nodes were harvested 12 hours after. The bar graph shows the percentage of tdTomato$^+$ cells in the spleen, peripheral and mesenteric lymph nodes as measured by flow cytometry. Data are represented as mean ± SD. Data are representative of 3 mice per condition and were analyzed by using an ordinary one-way ANOVA with Tukey's multiple comparisons test.



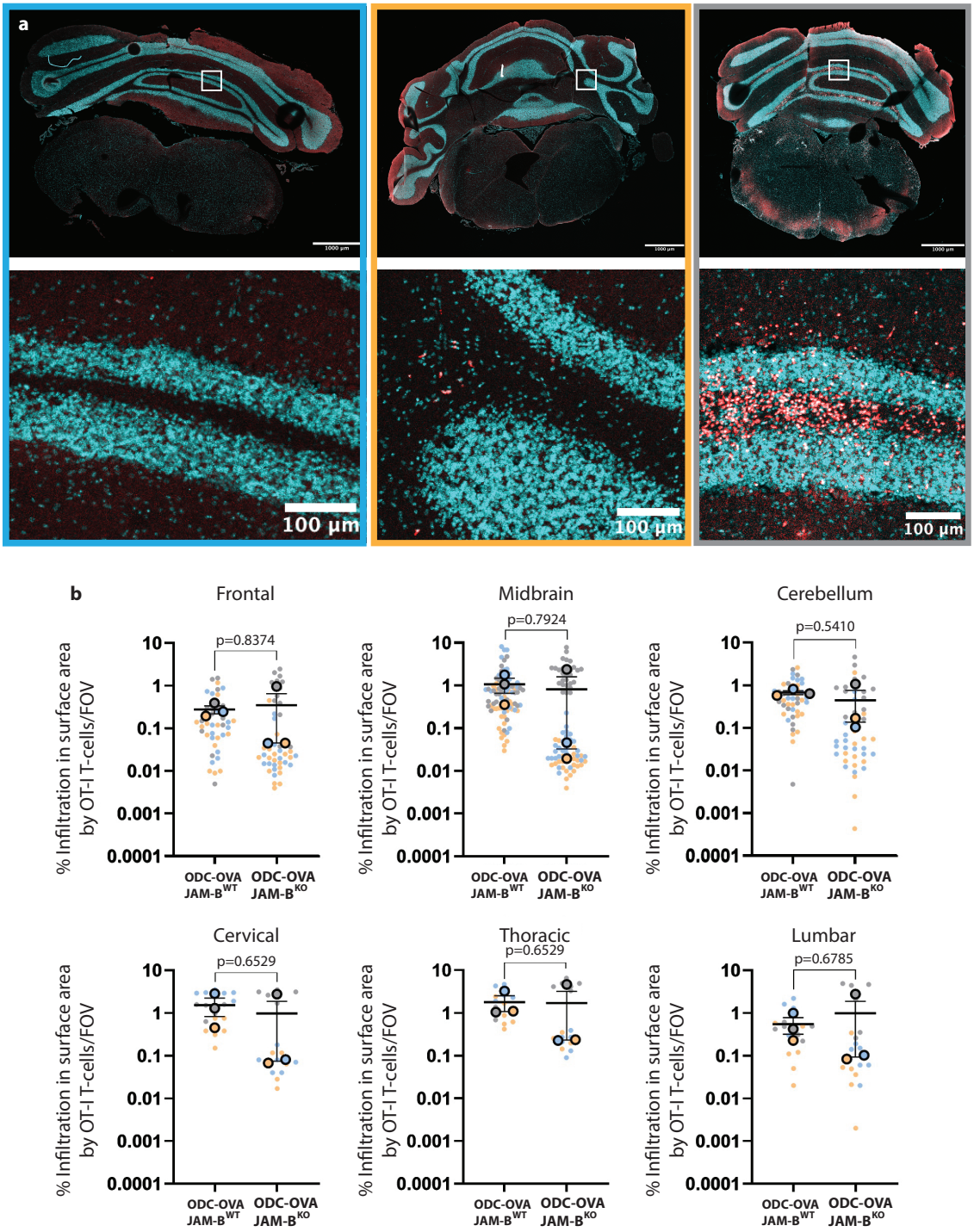
Supplementary Fig. 2 Gating strategy for CD45^{high} CD8^{+} T cell CNS immune cell infiltrates

Flow cytometry analysis of the CNS immune cell infiltrates from ODC-OVA; JAM-B^{WT} and ODC-OVA; JAM-B^{KO} mice on day 7 and 12 after LCMV-OVA infection. Single cells were selected by using forward scatter height versus forward scatter area (FSC- H::FSC-A) followed by live cell selection defined as the unstained population for the fixable viability dye (FVD780, Thermo Fischer, 65-0865-14). CNS infiltrating immune cells were next identified as CD45^{high} cells. Within this population CD8^{+} T cells were quantified. An according gating strategy was applied for CD45^{high} CD4^{+}, CD11b^{+} and CD11c^{+} cells, respectively.



Supplementary Fig. 3 CNS immune cell infiltrates in ODC-OVA; JAM-B^{WT} and ODC-OVA; JAM-B^{KO} mice at the end of the monophasic CD8 T cell mediated CNS autoimmune neuroinflammation

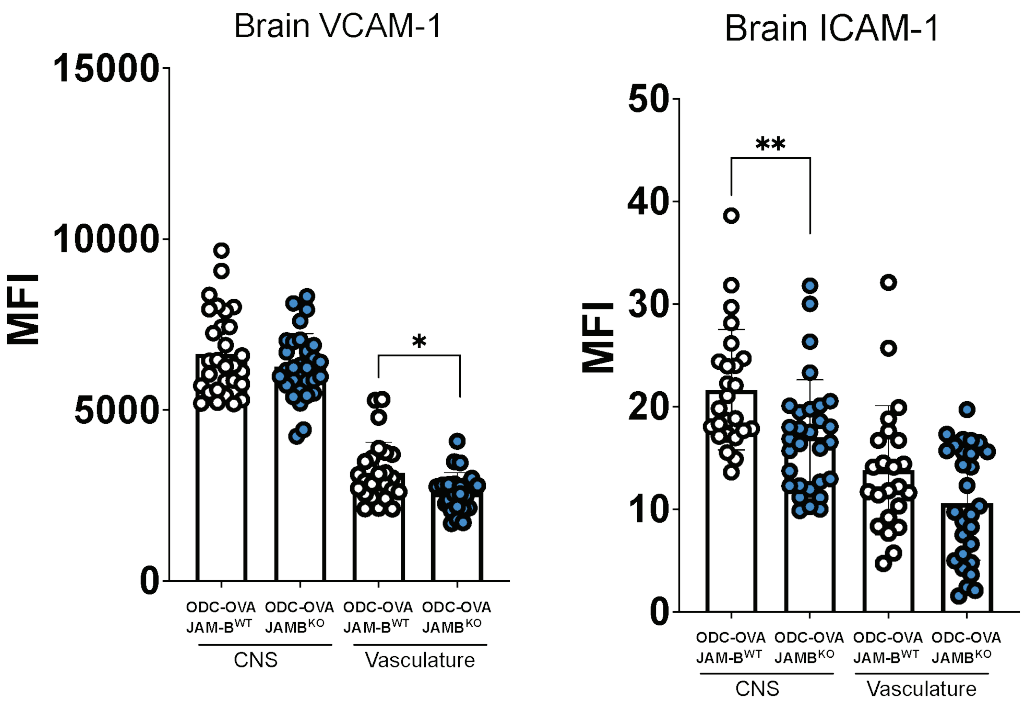
Flow cytometry analysis of CNS infiltrating immune cells isolated from brains and spinal cords of ODC-OVA;JAM-B^{WT} and ODC-OVA;JAM-B^{KO} mice at day 12 after LCMV-OVA infection. Quantification is shown as absolute numbers per organ of CD45^{high} infiltrating immune cells, CD8 T cells (CD45^{high} CD8^{+}), CD4 T cells (CD45^{high} CD4^{+}), monocytes/macrophages (CD45^{high} CD11b^{+}) and dendritic cells (CD45^{high} CD11c^{+}). Numbers are show as mean ± SD, where each dot represent one mouse. Data are representative of 5 mice per condition. Data were analyzed by using an ordinary one-way ANOVA with Tukey's multiple comparisons test.



Supplementary Fig. 4 High variability in the CNS infiltration of CD8 T cells in the absence of JAM-B during neuroinflammation

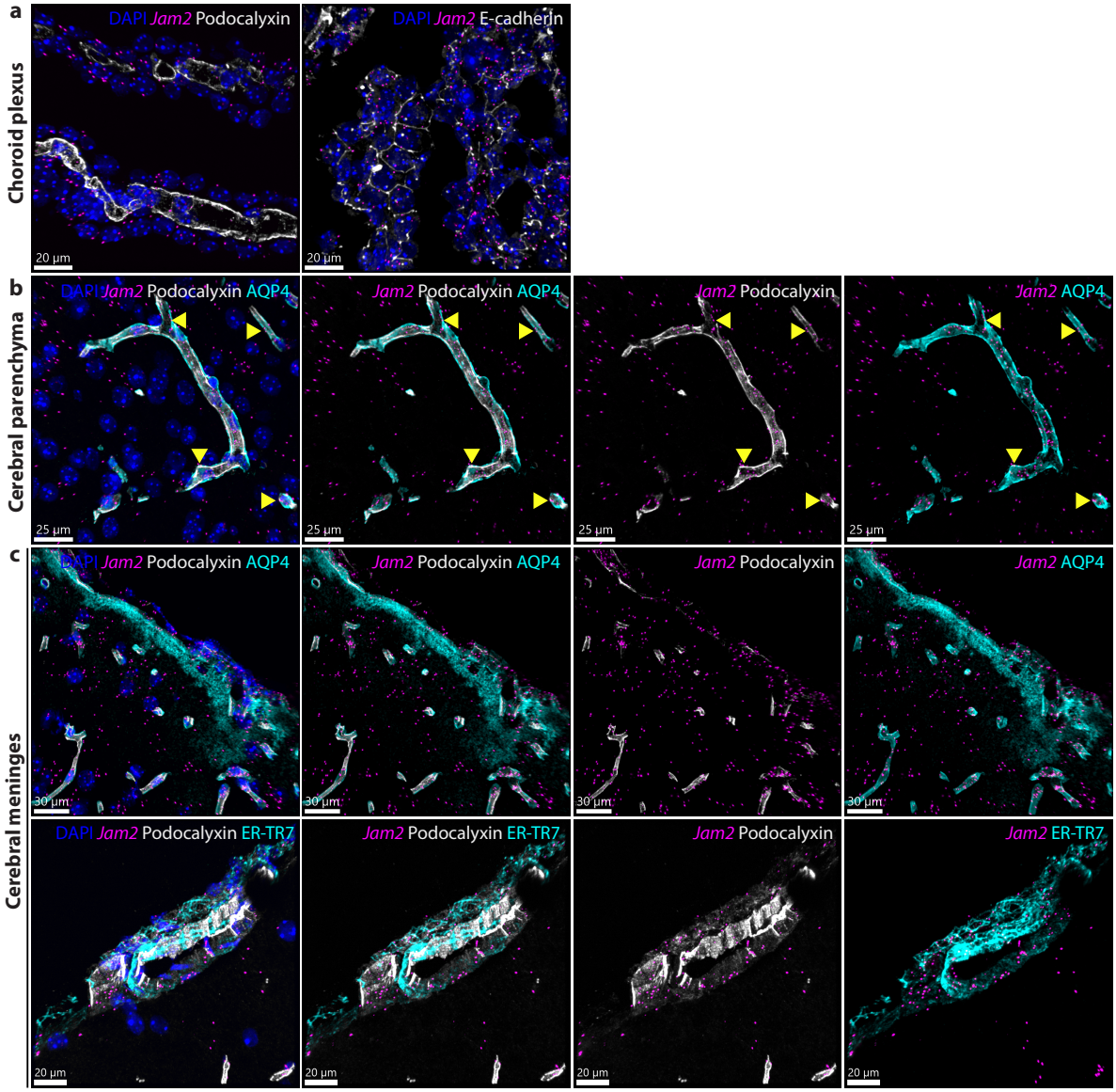
Naïve tdTomato$^+$ OT-I cells were adoptively transferred into ODC-OVA;JAM-B^{WT} and ODC-OVA;JAM-B^{KO} mice one day prior to LCMV-OVA infection. Brains and spinal cords were harvested on day 7 after LCMV-OVA infection. **a)** Representative maximum intensity projection images from 20 µm thick cryosections from the cerebellum of three different ODC-OVA;JAM-B^{KO} mice obtained by laser scanning confocal microscopy. Endogenous tdTomato$^+$ OT-I

cells are visible in red and DAPI (nuclei) is visible in blue. Data are representative of 5 mice. **b)** Percentage of surface area per field of view infiltrated by OT-I cells in the frontal and midbrain, cerebellum, and cervical, thoracic and lumbar spinal cord. Each dot without outline represent a single tissue section, and the outlined dots represent the mean value per mouse. Data from indivual mice are colour coded, matching the data from **a** (frame colour) and **b** (dot colour). A total of three mice per condition were analysed. Data were analysed based on the mean values per mouse using an ordinary two-sided parametric T test.



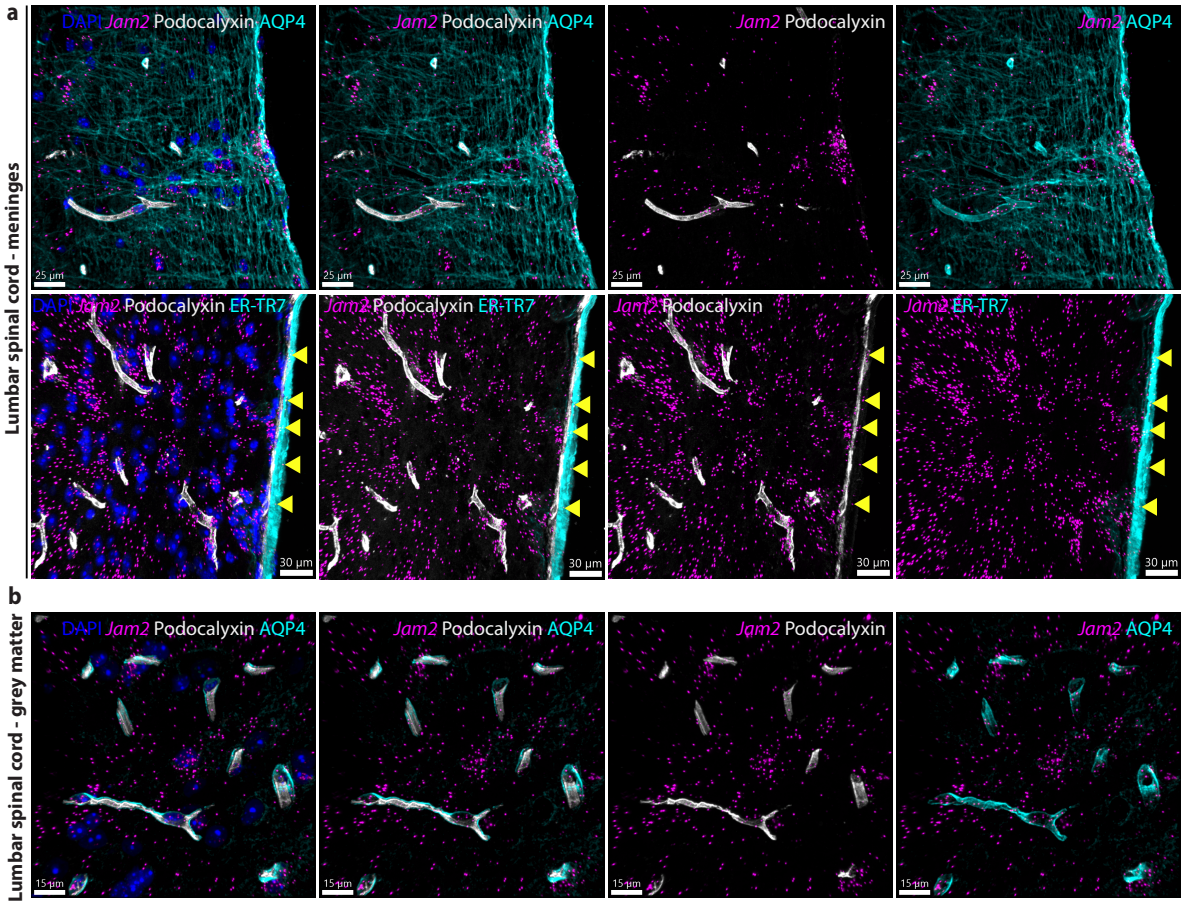
Supplementary Fig. 5 Expression of VCAM-1 and ICAM-1 in the brain of ODC-OVA; JAM-B^{WT} and ODC-OVA; JAM-B^{KO} mice

100 µm thick brain sections from ODC-OVA; JAM-B^{WT} and ODC-OVA; JAM-B^{KO} mice at day 7 after LCMV-OVA infection were co-immunostained for Podocalyxin and VCAM-1 or ICAM-1. Mean fluorescence intensity of VCAM-1 and ICAM-1 was measured on the whole spinal cord section and on the podocalyxin^{+} segemented vessels. Data are pooled from 3 independent experiments representing 3 mice per condition. Data are shown as mean ± SD and were analyzed using ordinary one-way ANOVA with Tukey's multiple comparisons test.



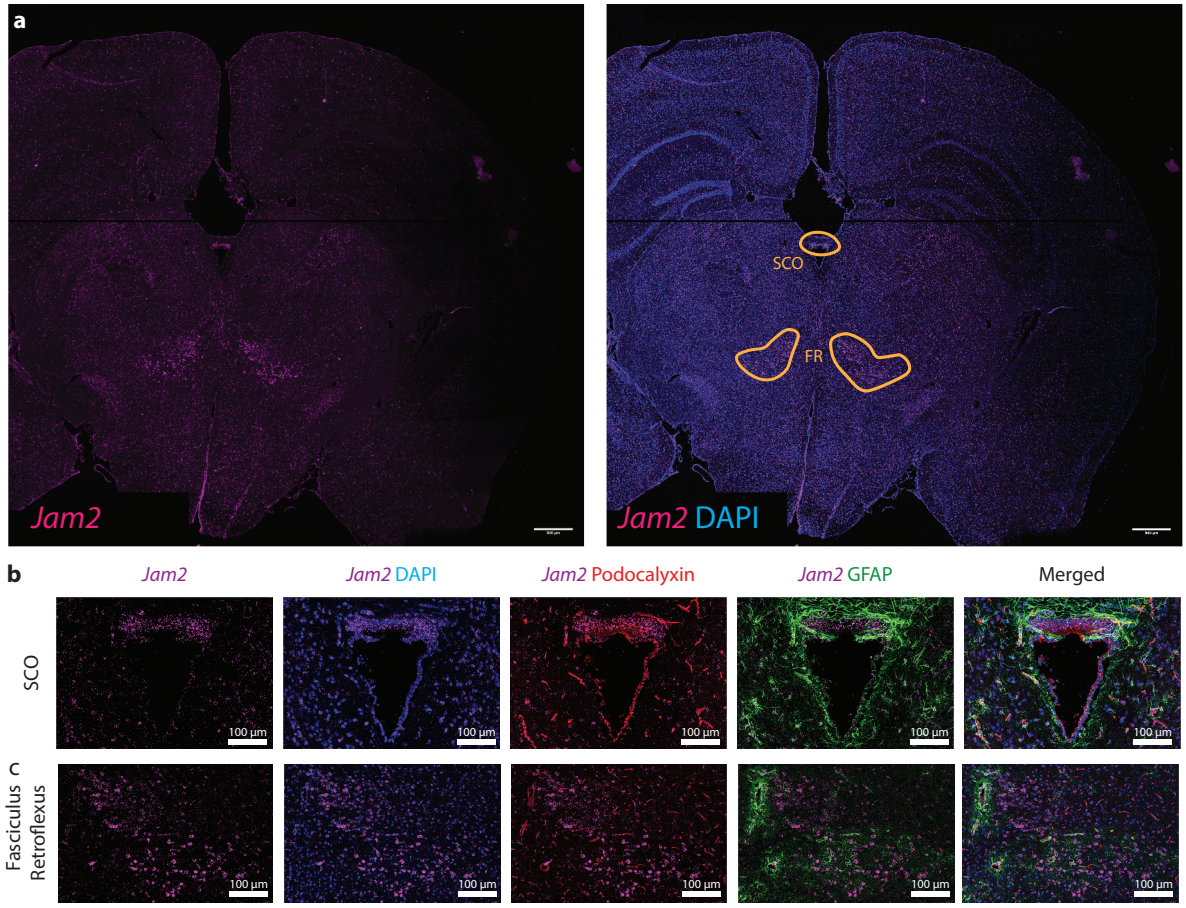
Supplementary Figure 6: *Jam2* expression in the brain

Jam2 RNAscope in situ hybridization (magenta) on 10 µm thick brain sections from healthy C57BL/6J mice coimmunostained for podocalyxin (white), aquaporin 4 (cyan), E-cadherin (white) and ER-TR7 (cyan). Nuclei (DAPI) are shown in blue. Representative maximum intensity projection images from the lateral and fourth ventricle choroid plexus **(a)**, the cerebral parenchyma **(b)** and the cerebral meninges **(c)** are shown. Yellow arrowheads in **(b)** mark the expression of *Jam2* at the abluminal aspect of the AQP4 immunostaining marking astrocyte endfeet. Data are representative of 2 independent experiments from 2 mice.



Supplementary Figure 7: *Jam2* expression in the spinal cord

Jam2 RNAscope in situ hybridization (magenta) on 10 µm thick spinal cord sections from healthy C57BL/6J mice coimmunostained for podocalyxin (white), aquaporin 4 (cyan), and ER-TR7 (cyan). Nuclei (DAPI) are shown in blue. Representative maximum intensity projection images from the meninges and white matter **(a)** and the grey matter of the spinal cord **(b)** are shown**.** Yellow arrowheads in **(a)** mark the expression of *Jam2* in ER-TR7-positive meningeal fibroblasts. Data are representative of 2 independent experiments from 2 mice.



Supplementary Fig. 8 *Jam2* is expressed in the mouse subcommissural organ and fasciculus retroflexus

a) *Jam2* RNAscope *in situ* hybridization (magenta) on 10 µm thick brain cryosections from ODC-OVA;JAM-B^{WT} mice. Nuclei (DAPI) are shown in blue. Orange shapes highlight the subcommissural organ (SCO) and fasciculus retroflexus (FR) of the mouse brain. Data are representative of 3 mice. **b-c)** *Jam2* RNAscope *in situ* hybridization (magenta) on 10 µm thick brain cryosections from the subcommissural organ (**b**) and fasciculus retroflexus (**c**) of ODC-OVA; JAM-B^{WT} mice coimmunostained for Podocalyxin (red) and GFAP (green). Nuclei (DAPI) are shown in blue. Data are representative of 3 mice.

Supplementary Table 1. Antibody list

Flow Cytometry Antibodies					
Antibody	**Clone**	**Species**	**Company**	**Cat number**	**Working concentration**
CD8-FITC	53-6.7	Rat	BioLegend	100706	10 µg/mL
CD11b-Pacific Blue	M1/70	Rat	BioLegend	101224	10 µg/mL
CD11c-BV605	N418	Armenian hamster	BioLegend	117333	10 µg/mL
CD4 AF700	RM4-5	Rat	BioLegend	100536	10 µg/mL
CD45 PE-Cy7	30-F11	Rat	BioLegend	103114	10 µg/mL
CD11a - eFluor450	M17/4	Rat	Invitrogen	48-0111-82	10 µg/mL
CD18 - PE	M18/2	Rat	BioLegend	302107	10 µg/mL
$\alpha 4\beta 7$ – eFluor710	DATK32	Rat	Invitrogen	46-5887-82	10 µg/mL
CD62L - APC	2PH1	Rat	BD Pharminogen	564310	10 µg/mL
CD49d - PE	R1-2	Rat	Invitrogen	12049281	10 µg/mL
Rat IgG2a – FITC	RTK2758	Isotype	BioLegend	400506	10 µg/mL
Rat IgG2b – Pacific Blue	RTK4539	Isotype	BioLegend	400627	10 µg/mL
Armenian Hamster IgG – BV605	HTK888	Isotype	BioLegend	400943	10 µg/mL
Rat IgG2b – AF700	RTK4530	Isotype	BioLegend	400628	10 µg/mL
Rat IgG2b – PE-Cy7	RTK4530	Isotype	BioLegend	400617	10 µg/mL

Immunofluorescence staining Antibodies					
Antigen	**Clone**	**Species**	**Company**	**Cat number**	**Working concentration**
Ovalbumin	Polyclonal	Rabbit	AbCam	AB181688	20 µg/mL
Olig2	Polyclonal	Goat	R&D Systems	AF2418	10 µg/mL
Laminin	Polyclonal	Rabbit	DAKO	Z0097	10 µg/mL
Podocalyxin	Polyclonal	Goat	R&D Systems	AF1556	2 µg/mL
GFAP	Polyclonal	Rabbit	DAKO	Z0334	20 µg/mL
Calbindin-D28k	Polyclonal	Rabbit	Proteintech	14479-1-AP	6 µg/mL
ICAM-1	25ZC7	Rat	In House	-	6 µg/mL
VCAM-1	2A11.12	Rat	In House	-	20 µg/mL
AQP4	Polyclonal	rabbit	Millipore	AB2218	10 µg/mL
E-Cadherin	Polyclonal	goat	R&D Systems	AF748	10 µg/mL
ER-TR7	Monoclonal	Rat	BMA Biomedicals	T-2109	2 µg/mL

Secondary Antibodies	Company	Cat number	Working concentration
Donkey polyclonal anti Goat IgG – AF647	Jackson Immuno Research	705-605-003	5 µg/mL
Donkey polyclonal anti Goat IgG – Cy3	Jackson Immuno Research	705-165-147	5 µg/mL
Donkey polyclonal anti Rat IgG – Cy5	Jackson Immuno Research	712-175-153	5 µg/mL
Donkey polyclonal anti Rabbit IgG – Cy5	Jackson Immuno Research	711-175-152	5 µg/mL
Donkey polyclonal anti Rabbit IgG – AF488	Thermo Fisher Scientific	A-21206	5 µg/mL
Donkey polyclonal anti Goat IgG – AF488	Thermo Fisher Scientific	A-11055	5 µg/mL

Function Blocking Antibodies					
Antigen	**Clone**	**Species**	**Company**	**Cat number**	**Working concentration**
JAM-B	150015	Rat	R&D Systems	MAB988	100 µg/mouse
VCAM-1	M/K-2.7	Rat	BioXCell	BE0027-5MG-A	250 µg/mouse
α4- integrin	PS/2	Rat	BioXCell	BE0071-5MG-A	250 µg/mouse
Rat IgG2a	R35-95	-	BD Pharmingen	553927	100 µg/mouse
Function Blocking Antibodies					
Antigen	**Clone**	**Species**	**Company**	**Cat number**	**Working concentration**
JAM-B	150015	Rat	R&D Systems	MAB988	100 µg/mouse
VCAM-1	M/K-2.7	Rat	BioXCell	BE0027-5MG-A	250 µg/mouse
α4- integrin	PS/2	Rat	BioXCell	BE0071-5MG-A	250 µg/mouse
Rat IgG2a	R35-95	-	BD Pharmingen	553927	100 µg/mouse